

**NASA  
Technical  
Paper  
2131**

April 1983

NASA  
TP  
2131  
c.1

# Effect of Flameholder Pressure Drop on Emissions and Performance of Premixed- Prevaporized Combustors

TECH LIBRARY KAFB, NM  
0134988

Robert A. Duerr  
and Valerie J. Lyons

LOAN COPY: RETURN TO  
AFWL TECHNICAL LIBRARY  
KIRTLAND AFB, N.M.



25th Anniversary  
1958-1983

**NASA  
Technical  
Paper  
2131**

1983

TECH LIBRARY KAFB, NM



0134988

# Effect of Flameholder Pressure Drop on Emissions and Performance of Premixed- Prevaporized Combustors

Robert A. Duerr  
and Valerie J. Lyons  
*Lewis Research Center  
Cleveland, Ohio*

**NASA**  
National Aeronautics  
and Space Administration  
**Scientific and Technical  
Information Branch**

Trade names or manufacturers' names are used in this report for identification only. This usage does not constitute an official endorsement, either expressed or implied, by the National Aeronautics and Space Administration.

## SUMMARY

Parametric tests were conducted to determine the effects of flameholder pressure drop on the emissions and performance of lean premixed-prevaporized combustors. A conical flameholder mounted in a diverging duct was tested with two values of flameholder blockage. Emissions of nitrogen oxides, carbon monoxide, carbon dioxide, and unburned hydrocarbons were measured for combustor entrance conditions of 600 to 800 K air temperature, 0.3- to 0.5-MPa pressure, and 20- to 35-m/sec reference velocity. Jet A fuel was injected at flow rates corresponding to an equivalence ratio range from 0.8 down to the lean stability limit. Emission results for the high-blockage flameholder were a substantial improvement over the low-blockage emission results. A correlation of combustion efficiency with flameholder pressure drop was developed for pressure drops less than 9 percent.

## INTRODUCTION

This report presents experimental results from a parametric study of the effects of flameholder pressure drop on the emissions and the performance of lean premixed-prevaporized combustors.

The NASA Lewis Research Center is engaged in advanced combustor research which includes investigating and establishing the technology to reduce exhaust emissions from gas turbine engines to environmentally acceptable levels over the entire subsonic flight regime while being consistent with the requirements for improved durability, performance, and fuel flexibility and with minimum adverse effects on weight and complexity. Emissions will be reduced by applying the lean premixed-prevaporized combustion technique along with variable combustor geometry. Possible benefits in addition to low emissions include (1) better control of the primary-zone equivalence ratio, leading to increased combustor liner life and increased turbine durability due to more uniform burning zones and burning at lower primary-zone equivalence ratios and (2) improved combustor altitude relight capability due to reduced airflow to the primary zone.

The technique of premixing the fuel and air before burning at lean equivalence ratios has been shown to be effective in reducing nitrogen oxides ( $\text{NO}_x$ ) emissions while maintaining high combustion efficiency (refs. 1 to 9). These studies used either propane or Jet A fuel in premixed systems with a variety of fixed flameholders such as perforated plates and cones.

Previous studies (refs. 10 and 11) in the area of flame stabilization in ramjets and afterburners indicated a strong correlation between flameholder geometry and combustion stability limits. Recent fundamental studies (refs. 7 and 8) in lean premixed systems demonstrated significant effects of flameholder geometry on combustion efficiency, combustor emissions, and stability limits.

Flameholder geometry affects combustor performance through pressure drop across the flameholder and mass entrainment behind the flameholder. The profile drag of the flameholder influences the degree of pressure drop, which controls the intensity of the primary zone turbulence. The rate of mass entrainment is related to the residence time within the recirculation region. The residence time influences the temperature and fuel-air mixture ratio limits beyond which combustion cannot be sustained and also has a measurable effect on rate-controlled parameters such as  $\text{NO}_x$  emissions.

The flameholder geometry also determines the downstream distance required for the flame to completely burn the unreacted gas mixture entering

the combustor. This effect is particularly significant in that it determines the combustor length necessary to achieve a given level of combustion efficiency. Anderson (ref. 1) showed that, by using lower equivalence ratios but longer residence times, it was possible to obtain good combustion efficiencies and low  $\text{NO}_x$  emissions. His data were taken with a perforated plate flameholder with 76-percent blockage.

From an economic viewpoint, combustor pressure drop presents significant cost tradeoff possibilities. With low pressure drop, relatively long combustors are required to achieve good efficiency. This increases the overall length, weight, and initial cost of the engine. High pressure drop enables use of a shorter combustor to achieve good efficiency. However, there will be a loss of thrust caused by the greatly increased power required to operate the compressor at high pressure ratios. Increases in pressure loss result in decreases in cycle efficiency. For example, an increase in combustor pressure drop from 5 to 6 percent results in an approximately 6-percent decrease in cycle efficiency (ref. 8), which significantly increases fuel consumption.

Flameholder pressure drop is thus a key area in the development of lean premixed-prevaporized systems. The flameholder pressure drop results from sudden contractions and expansions in flow areas and is a function of the flameholder geometry, the gas density, and the gas velocity in the contraction. The objective of the present investigation was to parametrically examine the effects of flameholder pressure drop on the performance of lean premixed-prevaporized combustors. Tests were conducted in a flame-tube rig by using a translating cone geometry to vary flameholder blockage. As the blockage increased, the pressure drop, turbulence, and recirculated volume also increased. The combustor was probed to determine pollutant emissions and combustion efficiency. Combustor test conditions were varied from an inlet air temperature of 600 to 800 K, an inlet pressure of 0.3 to 0.5 MPa, a reference velocity of 20 to 35 m/sec, and an equivalence ratio of 0.8 down to lean blowout using Jet A fuel.

## APPARATUS

The experiment was conducted in the closed-duct test facility shown in figure 1. Incoming air to the test section was preheated to temperatures from 600 to 800 K by a nonvitiating preheater. A contraction section was installed in the test rig to increase the flow velocity in the fuel-air mixing section. This served the trifold purpose of improving atomization of the fuel, reducing chances of flashback in the mixing section, and providing a convenient means of varying flameholder blockage. The inlet contraction section lowered the cross-sectional flow area from 83.5 to 22.9  $\text{cm}^2$  (diameter from 10.3 to 5.4 cm) in a length of 34 cm. The mixing-vaporizing tube was 5.4 cm in diameter, 23 cm in length, and ended in a 9.7-cm-long water-cooled diffuser cone to return the cross-sectional flow area to the original 83.5  $\text{cm}^2$ .

As shown in figure 1, the water-cooled combustor section was 10.3 cm in diameter, the same as the inlet duct, and 80 cm long. At the downstream end, high-pressure air was injected just upstream of a water-cooled 5-cm-diameter orifice plate. Sufficient air was injected to maintain combustor pressure at the desired level. After passing through the orifice plate, the gas stream was cooled by a water quench spray.

The translating conical flameholder was mounted in the diffuser cone at one of two axial positions to give a flameholder geometric blockage area

ratio of either 56 or 80 percent. Figure 2(a) schematically illustrates the hollow cone mounted in the diffuser at the 56- and 80-percent-blockage positions. The cone was 8.48 cm long and 5.00 cm in diameter at the base.

In one series of tests the flameholder and mixing tube were modified to allow water cooling in the interior of the cone as shown in figure 2(b). Concentric stainless steel tubing was used to bring water into the test rig through the mixing-vaporizing section. The flameholder was cooled by an impinging jet on the inside of the base of the cone; the outer tube removed the water from the cone to atmospheric exhaust.

To ensure good atomization, Jet A fuel was injected in the upstream direction through a cruciform fuel injector as shown in figure 3. It had one hole in the center which was 0.025 cm in diameter and three holes 0.079 cm in diameter on each of four 0.32-cm-diameter injector tubes.

Gas sampling of the combustion gases was accomplished by two sets of multipoint gas-sampling probes. Each set consisted of four water-cooled probes spaced 90° apart around the test section. Probe set 1 (designated probe 1) and probe set 2 (probe 2) were located 30 and 60 cm, respectively, downstream from the upstream end of the combustor section (see fig. 1); probe 2 was rotated 45° from the circumferential position of probe 1 in order to minimize wake interference effects. Each probe, as shown in figure 4, was 1.27 cm in diameter and had three ports of 0.165 cm in diameter located at centers of equal area in the circular test section. Stainless steel tubing (0.95 cm diam) connected the gas-sampling probes to the exhaust gas analyzers. To prevent condensation of unburned hydrocarbons, the sample line was steam-heated to a temperature between 410 and 450 K. The sample line was approximately 18 m long.

Gas-analysis equipment included a Model 402 Beckman flame-ionization detector for measuring unburned hydrocarbons, Model 315B Beckman nondispersive infrared analyzers for measuring concentrations of carbon monoxide (CO) and carbon dioxide (CO<sub>2</sub>), and a Model 10A Thermo-Electron chemiluminescent instrument for total NO<sub>x</sub> concentration. The instruments were calibrated with standard calibration gases at the beginning of each day's testing and whenever a range change was made.

Air inlet conditions were monitored using an array of three pitot tubes and five Chromel-Alumel thermocouples mounted upstream of the contraction section. Combustor exit pressures were measured by using the gas-sampling probes as total-pressure probes, that is, with zero gas-sample flow. Flameholder pressure drop was measured by a differential pressure transducer connected between the total-pressure ports on the entrance rake and the gas-sample line.

## MEASUREMENTS AND COMPUTATIONS

Reference conditions were based on the total airflow, the inlet air density using the total temperatures and pressure at the contraction section inlet, and the reference area (83.5 cm<sup>2</sup>), which is the cross-sectional flow area in the combustor.

The fuel-air ratio was determined both by metering the fuel and air flow rates and by making a carbon balance from the measured concentrations of CO, CO<sub>2</sub>, and unburned hydrocarbons. Sample validity was checked by comparing the two methods, and only those points whose metered and calculated fuel-air ratios varied by no more than 15 percent are included in this report.

The emissions were measured as concentrations in parts per million (ppm) by volume and converted to an emission index EI by using the equation

$$EI_n = \frac{C_n}{1000} \frac{M_n}{M_{mix}} \frac{1+f}{f} \quad (1)$$

where

$EI_n$  = emission index of species n  
 $C_n$  = concentration of n, ppm  
 $M_n$  = molecular weight of n  
 $M_{mix}$  = molecular weight of mixture  
 $f$  = fuel-air weight ratio

Combustion inefficiency I was determined by exhaust gas analysis by using the equation (ref. 12)

$$I = \frac{EI_{HC}}{10} + \frac{EI_{CO} - EI_{CO, eq}}{42.7}$$

where  $EI_{HC}$  and  $EI_{CO}$  are the emission index values for unburned hydrocarbons and CO based on gas analysis fuel-air ratio and  $EI_{CO, eq}$  is the equilibrium level of CO emissions.

The total pressure loss which results from sudden expansions and contractions in flow area can be expressed as (ref. 7)

$$\frac{\Delta P}{P} = k \frac{\gamma}{2} M_{max}^2$$

where  $k$  is a resistance coefficient which is solely a function of the system geometry,  $\gamma$  is the specific heat ratio, and  $M_{max}$  is the highest Mach number achieved in the contraction based on the area ratio and mass flow. Values of  $M_{max}$  are obtained by using the equation

$$M_{max} = \frac{M_{ref}}{1-B/1000}$$

where  $M_{ref}$  is the reference Mach number and  $B$  is the flameholder blockage (in percent). For this report, flameholder blockage is defined as the ratio of the total blocked area at the station where the base of the flameholder is located to the reference area of the combustor. Blockage ratios of 56 and 80 percent were used in this study.

Tests were conducted by the method described in reference 9 to determine the fuel vaporization and fuel-air uniformity at the flameholder station. Results indicated better than 95 percent vaporization of the fuel, and fuel-air ratio variation was less than 10 percent across the duct.

## RESULTS AND DISCUSSION

Experiments were conducted at inlet air temperatures of 600 to 800 K, pressures of 0.3 and 0.5 MPa, reference velocities of 20 to 35 m/sec, and equivalence ratios of 0.8 down to lean blowout using Jet A fuel. Table I

shows a matrix of the conditions tested and experimental limitations with a directory of data figures and flameholder pressure drops (in percent) for each condition. The effect of combustor residence time on emissions was studied by comparing gas-sample data from probe 1 (30 cm downstream of the flameholder) and probe 2 (60 cm downstream of the flameholder).

## EMISSIONS

Combustion inefficiency, as defined in the previous section, is a function of emissions of unburned hydrocarbons and excess CO above equilibrium levels. Unburned hydrocarbons are formed early in the combustion process and are readily oxidized to CO. Thus the primary contributor to inefficiency is CO. Interpreting the data in this study, the reader may find it helpful to think of high inefficiency as being a result of high CO emissions. Hydrocarbon oxidation kinetics necessarily produce a large amount of CO as an intermediate, which must then be consumed in order to achieve high efficiency. Reacting oxygen and nitrogen present in the primary zone produces  $\text{NO}_x$ . Its formation is favored by the reactive conditions which favor CO consumption, namely, high temperature, long residence time, and high pressure. The consequence of the CO and  $\text{NO}_x$  formation processes is that conditions or combustor design changes which decrease  $\text{NO}_x$  emissions generally increase combustion inefficiency and vice versa. Thus it is important to examine both parameters in order to assess combustor performance properly. A more detailed discussion of this tradeoff is contained in reference 13.

Results showing the effects of combustor length (or residence time) and equivalence ratio on emissions of  $\text{NO}_x$  and on combustion inefficiency are presented in figures 5 to 12 for ranges of flameholder blockage, inlet pressure, inlet air temperature, and reference velocity (see table I). Data are presented as emission indices of  $\text{NO}_x$  and percent inefficiency as functions of equivalence ratio as calculated from the gas sample. In this set, all the data are presented separately for each inlet condition. Comparisons of some of the data presented in figures 5 to 12 are cross plotted in figures 13 to 15 for specific parameters of interest: flameholder blockage, inlet pressure, and water cooling of the conical flameholder. Data in these figures present an emissions map of  $\text{NO}_x$  emissions and combustion inefficiency for each of the two gas-sample locations.

The general trends of the data presented in figures 5 to 12 are similar, although absolute levels of  $\text{NO}_x$  and combustion inefficiency vary from figure to figure. In general, the data indicate that  $\text{NO}_x$  emissions increase with increases in equivalence ratio, inlet air temperature, and combustor residence time. Combustion inefficiency generally decreases with increases in equivalence ratio, inlet air temperature, and combustor residence time. These trends suggest that, if  $\text{NO}_x$  emissions were plotted against combustion inefficiency and a line was faired through the data points, the instantaneous slope of that line would generally be negative over the range of data. Since combustors are designed with the goal of minimizing combustion inefficiency and  $\text{NO}_x$  emissions, the best design tradeoff is to achieve as many data points close to the origin as possible. This principle is used in comparing the data presented in figures 13 to 15, where the ordinate is the  $\text{NO}_x$  emissions in g/kg fuel and the abscissa is combustion inefficiency, which is mostly an indication of the amount of CO emissions present, as discussed previously.

Flameholder blockage. - Figure 13 presents a comparison of typical emissions (mainly  $\text{NO}_x$  and CO) results for the two flameholder blockages.



The data in this figure were taken at the two probe locations, an inlet pressure of 0.3 MPa and 35-m/sec reference velocity. Results indicate that the emissions with the high-blockage flameholder, with its corresponding high-pressure loss, represent a substantial improvement over the emissions of the low-blockage flameholder at both sampling locations and for both inlet air temperatures.

The expected decrease in combustion inefficiency and increase in NO<sub>x</sub> emissions, observed in comparing figure 13(b) with 13(a), is due to the increase in residence time of the combustion gases.

Combustion pressure. - A comparison of typical emission results for the two combustor pressures tested, 0.3 and 0.5 MPa, is shown in figure 14. The data were taken at a reference velocity of 25 m/sec using the high-blockage flameholder configuration. As can be seen from the data, the increase in combustor pressure decreases the combustion inefficiency and leaves the NO<sub>x</sub> emissions relatively unchanged.

Water-cooled cone. - The effect of a water-cooled flameholder on emissions is shown in figure 15 for a combustor pressure of 0.5 MPa, a reference velocity of 25 m/sec, and the high-blockage flameholder. The data indicate that water cooling has a deleterious effect on the combustion efficiency. The efficiency does not improve significantly with additional burning length, which implies that water cooling lowered the temperature of the incoming fuel-air mixture to the combustor. Some of the vaporized fuel may even have recondensed on the surface of the cone. Heat balance calculations indicate a cooling of the incoming fuel-air mixture of approximately 40 K. This would lead to shedding droplets of fuel from the downstream end of the cone; resultant incomplete burning of these droplets could lead to the relatively high level of hydrocarbon emissions measured in these tests. There was no attempt to study the influence of water flow rate on emissions.

Reference velocity. - Comparison of data at two reference velocities (25 and 35 m/sec) showed little effect of reference velocity on emissions.

#### Flameholder Pressure Drop

The experimental values of flameholder pressure drop determined during the testing are shown in figure 16 as a function of flameholder Mach number  $M_{max}$ . The values of pressure drop shown in the figure represent the mean of a number of data points taken at each condition. No data for the water-cooled flameholder are shown because of the presence of the additional waterline tubing in the mixer-vaporizer section, which led to higher pressure drops.

The line drawn through the data represents a least-squares curve fit of the data given by the equation

$$\frac{\Delta P}{P} = 1.62 \frac{\gamma}{2} M_{max}^2$$

Thus the value of  $K$ , the resistance coefficient for this study, is 1.62, compared with 1.5 suggested in reference 7 for a similar configuration.

A compilation of results illustrating the tradeoff between flameholder pressure drop and combustion efficiency is shown in figure 17. Combustion inefficiency is plotted as a function of flameholder pressure drop (both expressed as percent) for an equivalence ratio of 0.6, inlet pressures of 0.3 and 0.5 MPa, inlet air temperatures of 600 to 800 K, and both probe positions as indicated by the various symbols. Data for both probes 1 and 2

form a roughly V-shaped pattern with a minimum in the 8 to 10 percent pressure drop range. The data below 9-percent pressure drop are of interest to the combustion system designer since they represent the area of practical economic design. The equations for the two lines shown in figure 17 relating combustion inefficiency I and pressure drop  $\Delta P/P$  for each probe are

Probe 1

$$I = 30 e^{-0.5 \Delta P/P}$$

Probe 2

$$I = 15 e^{-0.5 \Delta P/P}$$

with I and  $\Delta P/P$  both expressed as percent. These correlations are based solely on the data in this report; however, the similarity of the slopes indicates a general trend independent of axial position.

A similar comparison of  $\text{NO}_x$  emissions and flameholder pressure drop is shown in figure 18. The  $\text{NO}_x$  emission index is plotted as a function of pressure drop for an equivalence ratio of 0.6. For both inlet air temperatures of 700 and 800 K,  $\text{NO}_x$  emissions increase with increasing flameholder pressure drop. This result is consistent with the combustion inefficiency decrease with increasing flameholder pressure drop shown in figure 17. The tradeoff between high  $\text{NO}_x$  and high combustion inefficiency (due to CO) is again evident.

#### Lean Stability Limits

The experimental lean stability limits determined during the test series are expressed as equivalence ratios in table II. The data that were obtained show that the lean stability limit is decreased, or improved, by increases in inlet air temperature and flameholder blockage. Reference velocity had a mixed effect on the lean stability limit. For the low-blockage tests, increasing reference velocity caused a significant decrease in the blowout equivalence ratio, while for the high-blockage tests, increasing reference velocity slightly increased the blowout equivalence ratio. Results from limited tests with the water-cooled cone indicate higher blowout equivalence ratios than those with an uncooled cone. The values for lean stability limits shown in table II are averages of at least two blowout tests at each point. Like most instability phenomena, the lean stability limit is somewhat erratic and did not accurately reproduce from one test to another.

#### SUMMARY OF RESULTS

Parametric tests were conducted to determine the effects of flameholder pressure drop on the emissions and performance of lean premixed-prevaporized combustors. A translating conical flameholder mounted in a diverging duct was tested at two values of flameholder blockage. Emissions of nitrogen oxides ( $\text{NO}_x$ ), carbon monoxide (CO), carbon dioxide ( $\text{CO}_2$ ), and unburned hydrocarbons were measured for combustor entrance conditions of 600 to 800 K air temperature, 0.3- and 0.5-MPa pressure, and of 20- to 35-m/sec reference velocity. Jet A fuel was injected at flow rates corresponding to an equiv-

alence ratio range from 0.8 down to the lean stability limit. The results of the test program are summarized as follows:

1. The overall emissions performance of the high-blockage flameholder was an improvement over that obtained with the low-blockage flameholder.

2. An increase in combustor pressure improved the combustion efficiency and had a relatively small effect on  $\text{NO}_x$  emissions.

3. Water cooling of the conical flameholder had a deleterious effect on the combustor efficiency because of an apparent decrease in the temperature of the incoming fuel-air mixture to the combustor. This effect also resulted in a significant increase in the equivalence ratio at the lean stability limit.

4. A correlation of combustion efficiency with flameholder pressure drop was developed as a function of combustor length for pressure drops less than 9 percent.

5. As expected, increasing the combustor residence time increased  $\text{NO}_x$  emissions and increased combustor efficiency.

Lewis Research Center  
National Aeronautics and Space Administration  
Cleveland, Ohio, October 8, 1982

#### REFERENCES

1. Anderson, D.: Effects of Equivalence Ratio and Dwell Time on Exhaust Emissions for an Experimental Premixing, Pre vaporizing Burner. ASME Paper 75-GT-69, Mar. 1975.
2. Roffe, Gerald; and Ferri, Antonio: Pre vaporization and Premixing to Obtain Low Oxides of Nitrogen in Gas Turbine Combustors. NASA CR-2495, Mar. 1975.
3. Fletcher, Ronald S.; and Heywood, John B.: A Model for Nitric Oxide Emission from Aircraft Gas Turbines. AIAA Paper 71-123, Jan. 1971.
4. Roffe, Gerald; and Ferri, Antonia: Effect of Premixing Quality on Oxides of Nitrogen in Gas Turbine Combustors. NASA CR-2657, Feb. 1976.
5. Spadaccini, L. J.; and Szetela, E. J.: Approaches to the Pre vaporized-Premixed Combustor Concept for Gas Turbines. ASME Paper 75-GT-85, Mar. 1975.
6. Marek, Cecil J.; and Papathakos, Leonidas C.: Exhaust Emissions From a Premixing, Pre vaporizing Flame Tube Using Liquid Jet A Fuel. NASA TM X-3383, Apr. 1976.

7. Roffe, Gerald; and Venkataramani, J. S.: Experimental Study of the Effects of Flameholder Geometry on Emissions and Performance of Lean Premixed Combustors. (GASL-TR-249, General Applied Science Labs, Inc.; NASA Contract NAS3-20603.) NASA CR-135424, June 1978.
8. McVey, J. B.; and Kennedy, J. B.: Lean Stability Augmentation Study. (UTRC/R79-914104-18, United Technologies Research Center; NASA Contract NAS3-20804.) NASA CR-159536, May 1979.
9. Cooper, Larry P.: Effect of Degree of Fuel Vaporization Upon Emissions for a Premixed Partially Vaporized Combustion System. NASA TP-1582, Jan. 1980.
10. Barnett, Henry C.; and Hibbard, Robert E., eds.: Adaptation of Combustion Principles to Aircraft Propulsion. Volume II - Combustion in Air-Breathing Jet Engines. NACA RM E55G28, 1956.
11. Ozawa, R. I.: Survey of Basic Data on Flame Stabilization and Propagation for High Speed Combustion Systems. AFAPL-TR-70-81, Marquardt Corp., January 1970. (AD-880322.)
12. Biaglow, J. A.; and Trout, A. M.: Effect of Flame Stabilizer Design on Performance and Exhaust Pollutants of a Two-Row 72-Module Swirl-Can Combustor. NASA TM X-3373, Mar. 1976.
13. Verkamp, F. J.; Verdouw, A. J.; and Tomlinson, J. G.: Impact of Emission Regulations on Future Gas Turbine Engine Combustors. Aircr., vol. 11, no. 6, June 1974, pp. 340-344.

TABLE I. - TEST MATRIX AND FIGURE MAP WITH FLAMEHOLDER PRESSURE DROP

[Pressure drop in percent.]

Reference velocity, $V_{ref}$ , m/sec	Low blockage			High blockage			High blockage			High blockage, water-cooled		
	Inlet air pressure, MPa											
	0.3						0.5					
	Inlet temperature, T, K											
	600	700	800	600	700	800	600	700	740	600	700	740
20	(a)	(a)	(a)	(a)	(a)	(a)	(a)	(a)	(a)	(a)	fig. 11 3.2	(b)
25	(a)	(a)	(a)	fig. 7 7.6	fig. 7 6.0	fig. 7 6.1	fig. 9 6.7	fig. 9 9.2	fig. 9 8.0	fig. 12 5.2	fig. 12 5.9	(b)
30	fig. 5 2.7	fig. 5 4.0	fig. 5 2.3	(b)	(b)	(b)	fig. 10 7.1	(c)	(c)	(b)	(c)	(c)
35	(c)	fig. 6 4.1	fig. 6 3.2	(c)	fig. 8 13.3	fig. 8 10.0	(c)	(c)	(c)	(c)	(c)	(c)

<sup>a</sup>Instability due to autoignition/flashback phenomena.

<sup>b</sup>Not tested.

<sup>c</sup>Facility airflow limited.

TABLE II. - LEAN STABILITY LIMITS

[Limits expressed as equivalence ratio.]

Reference velocity, $V_{ref}$ , m/sec	Low blockage			High blockage			High blockage			High blockage, water-cooled		
	Inlet air pressure, MPa											
	0.3						0.5					
	Inlet temperature, T, K											
	600	700	800	600	700	800	600	700	740	600	700	740
20	---	---	---	---	---	---	---	---	---	---	0.34	---
25	---	---	---	0.37	0.32	0.29	0.32	0.36	0.36	0.39	.42	---
30	0.60	0.54	0.48	---	---	---	.35	---	---	---	---	---
35	---	.41	.36	---	.34	.31	---	---	---	---	---	---

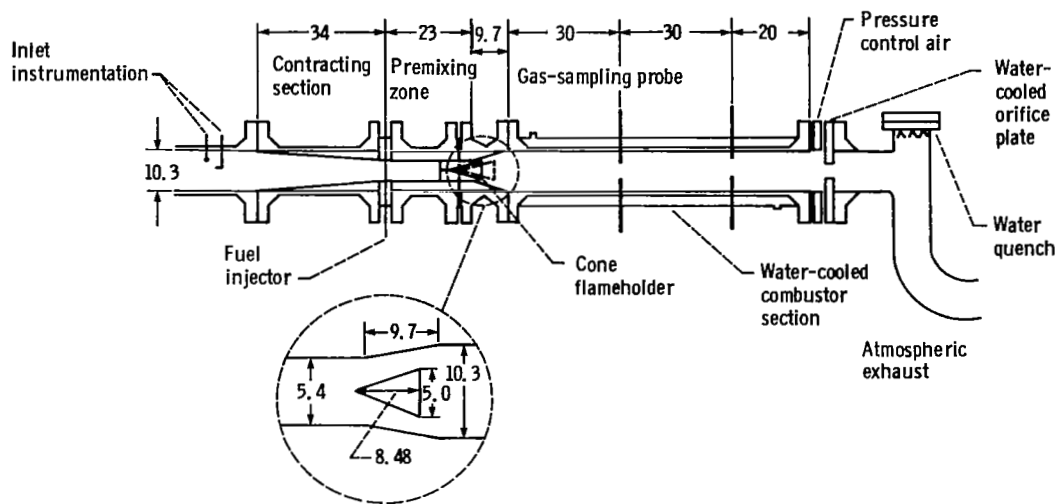
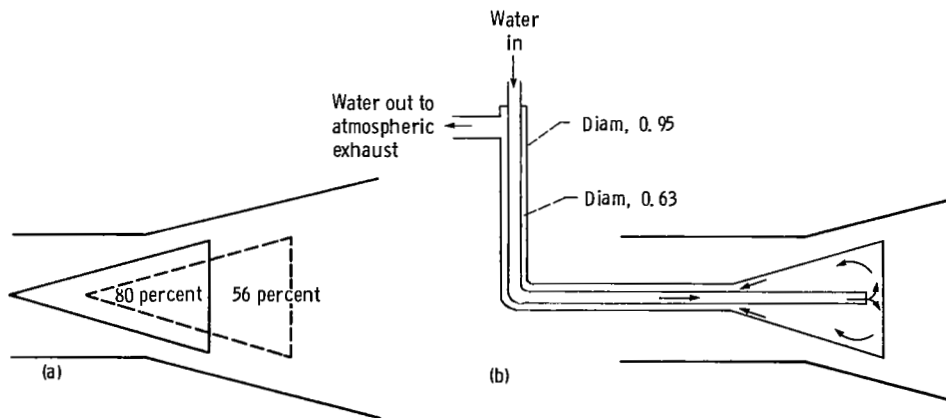


Figure 1. - Test rig (dimensions in cm).



(a) Flameholder positions.

(b) Water-cooling layout.

Figure 2. - Conical flameholder as installed in test rig (dimensions in cm).

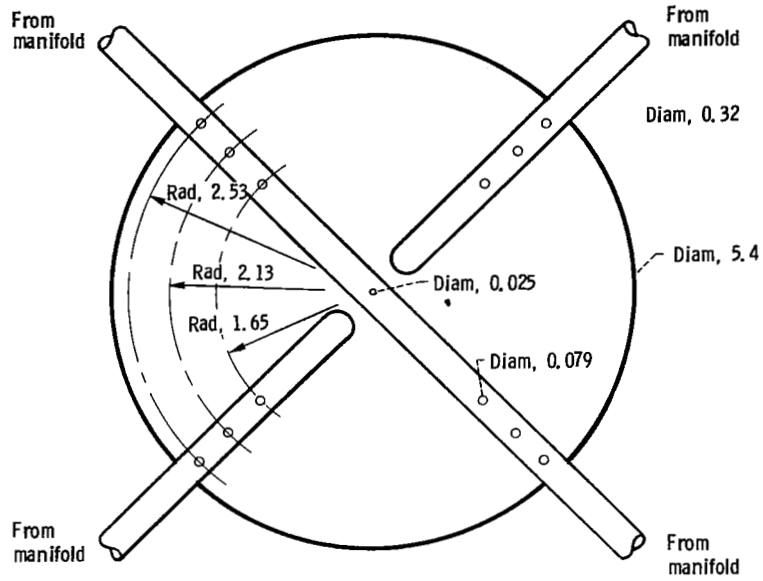


Figure 3. - Fuel injector, View looking downstream (dimensions in cm).

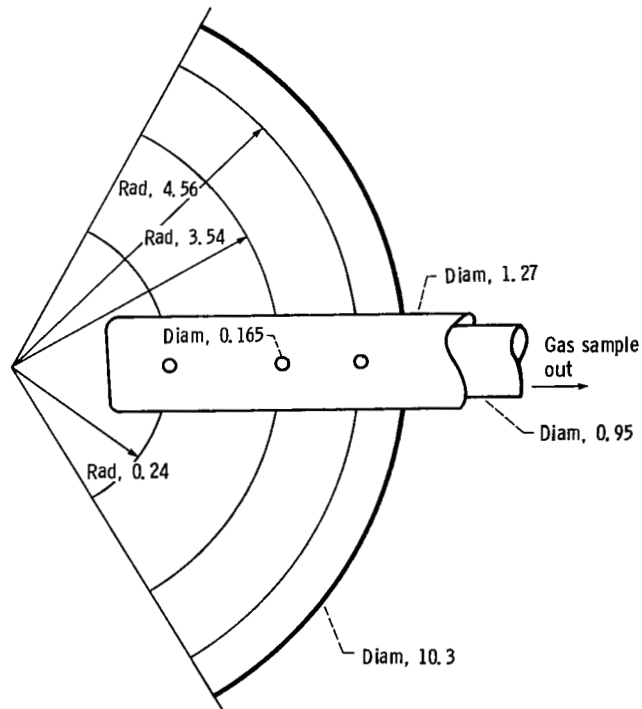


Figure 4. - Water-cooled gas-sampling probe (dimensions in cm).

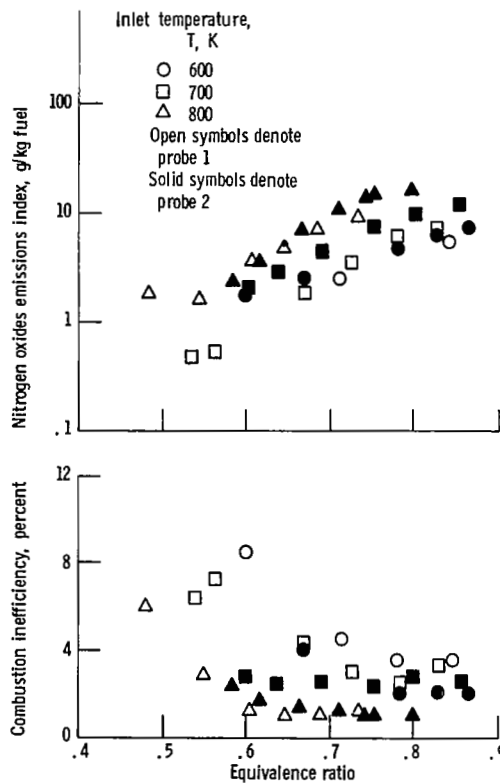


Figure 5. - Emission results for low-blockage flameholder. Inlet air pressure, 0.3 MPa; reference velocity, 30 m/sec.

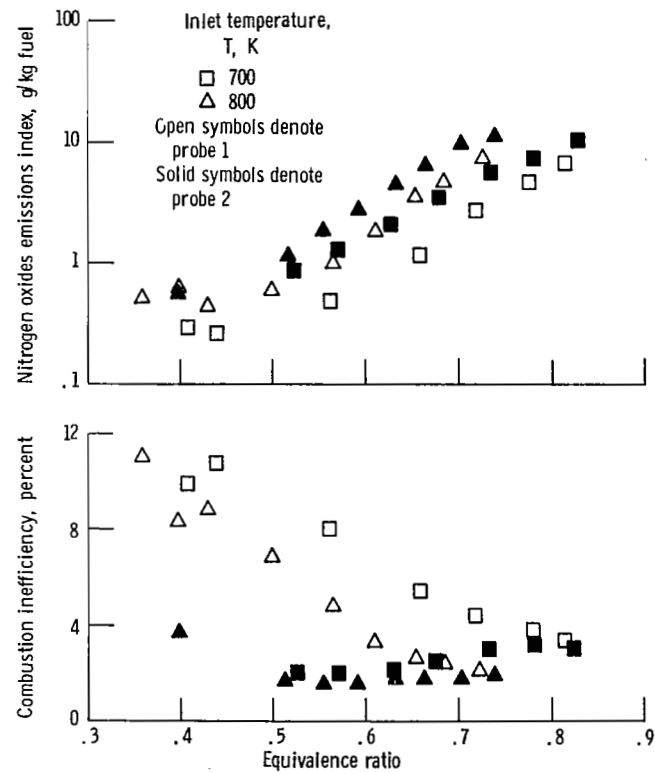


Figure 6. - Emission results for low-blockage flameholder. Inlet air pressure, 0.3 MPa; reference velocity, 35 m/sec.



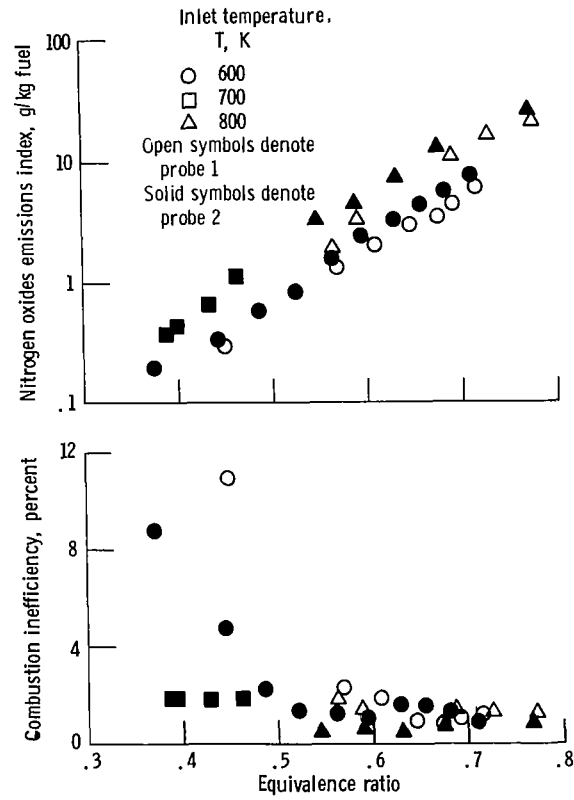


Figure 7. - Emission results for high-blockage flameholder. Inlet air pressure, 0.3 MPa; reference velocity, 25 m/sec.

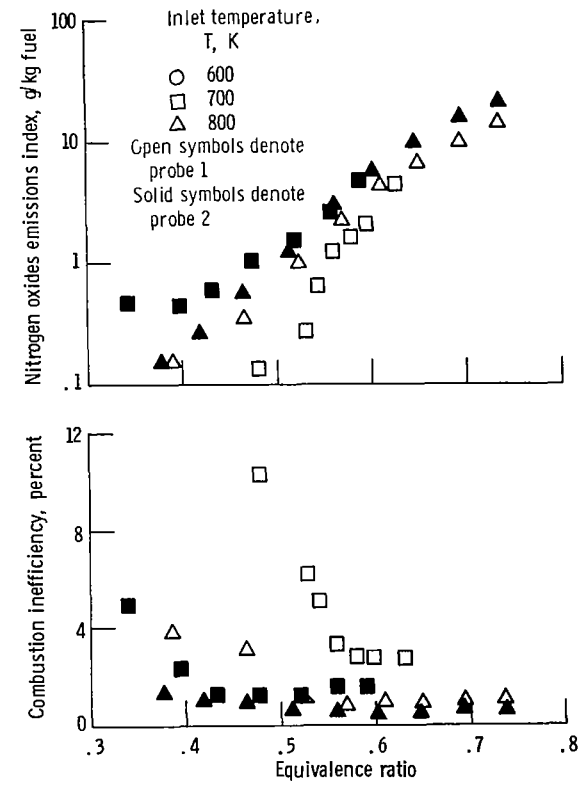


Figure 8. - Emission results for high-blockage flameholder. Inlet air pressure, 0.3 MPa; reference velocity, 35 m/sec.

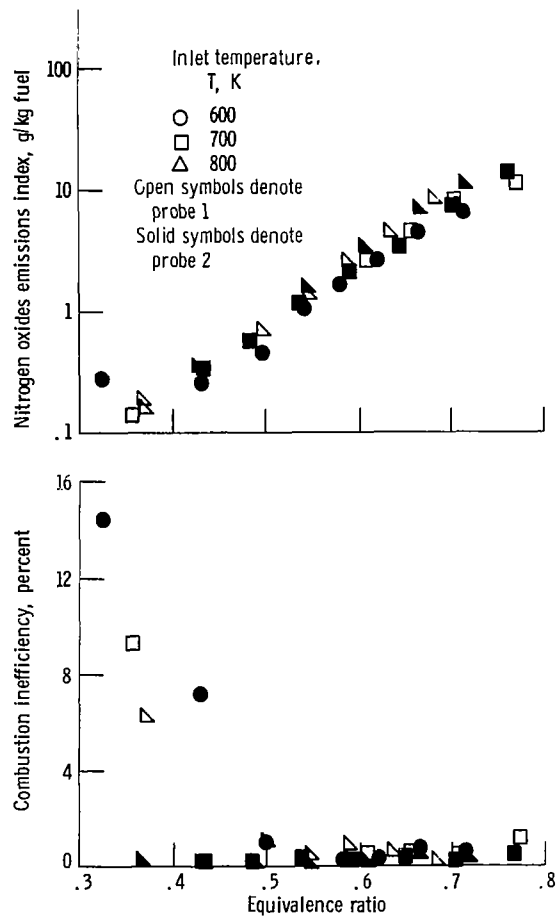


Figure 9. - Emission results for high-blockage flameholder. Inlet air pressure, 0.5 MPa; reference velocity, 25 m/sec.

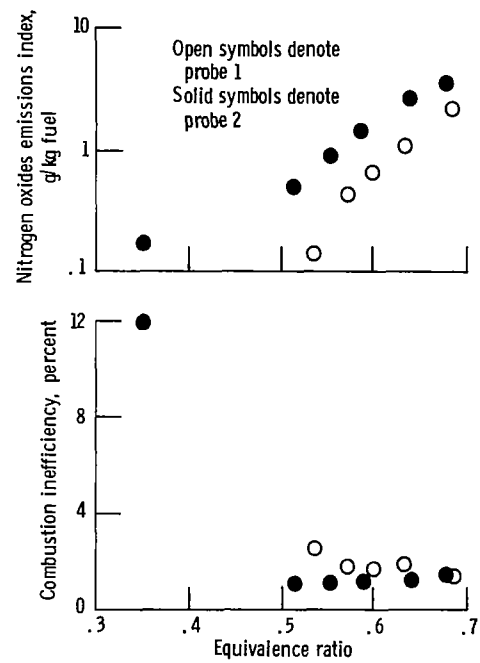


Figure 10. - Emission results for high-blockage flameholder. Inlet air pressure, 0.5 MPa; reference velocity, 30 m/sec; inlet temperature,  $T$ , 700 K.

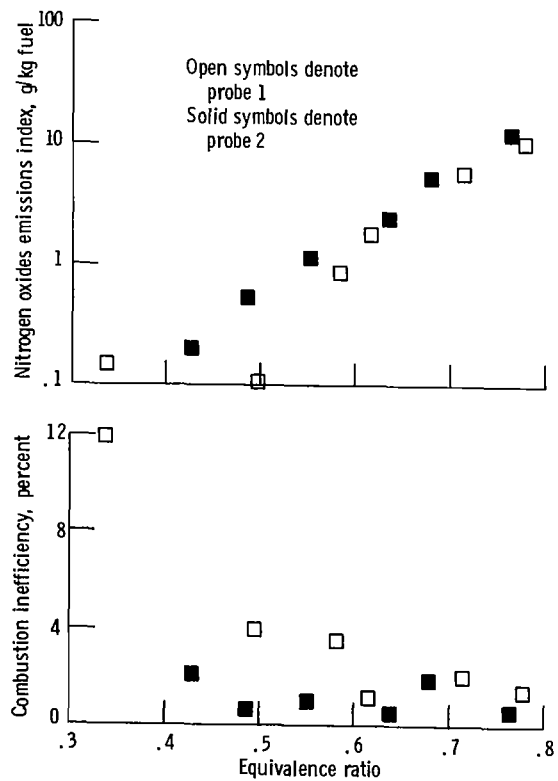


Figure 11. - Emission results for high-blockage, water-cooled flameholder. Inlet air pressure, 0.5 MPa; reference velocity, 20 m/sec; inlet temperature, T, 700 K.

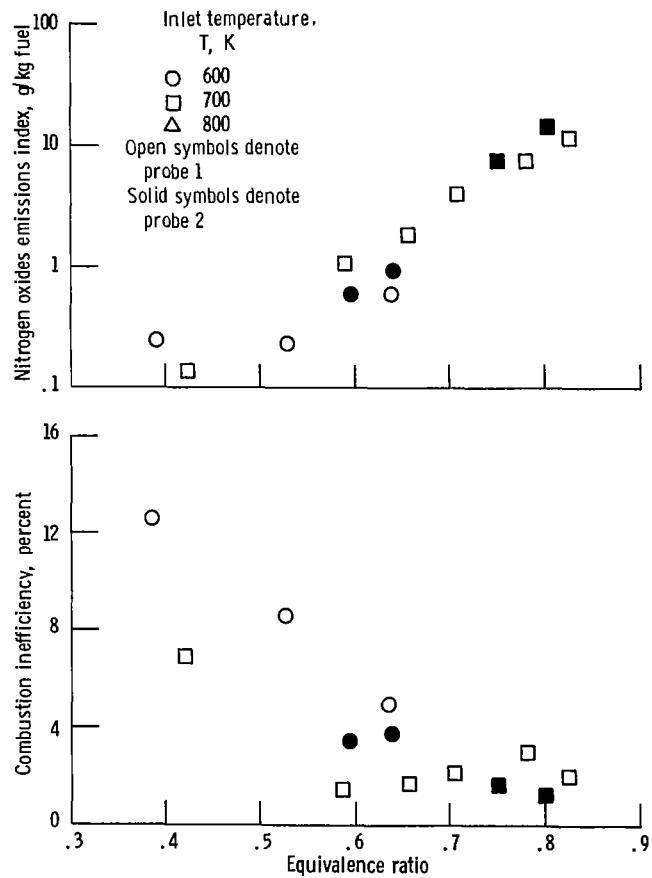


Figure 12. - Emission results for high-blockage, water-cooled flameholder. Inlet air pressure, 0.5 MPa; reference velocity, 25 m/sec.

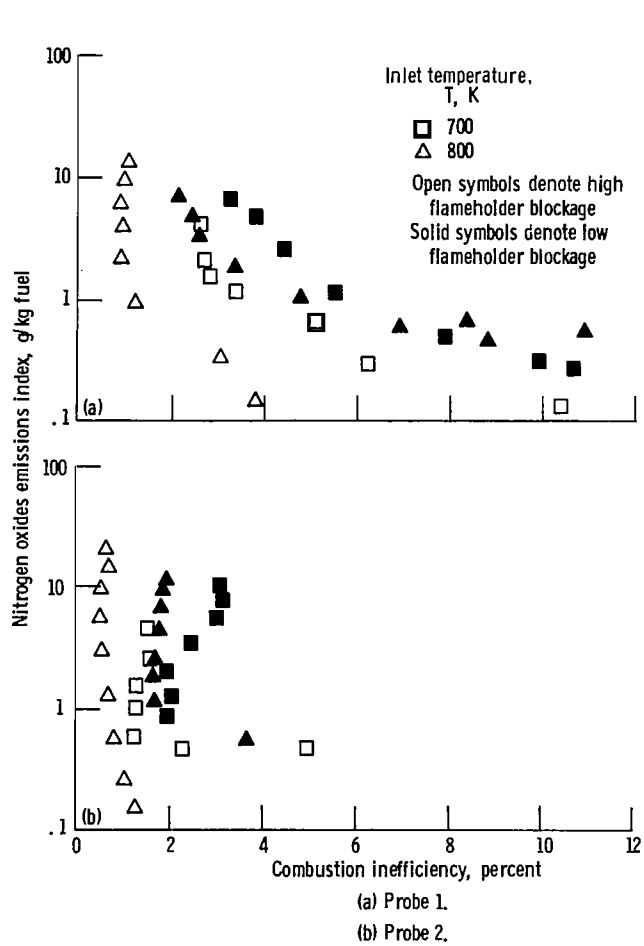


Figure 13. - Effects of flameholder blockage on emissions results. Inlet air pressure, 0.3 MPa; reference velocity, 35 m/sec.

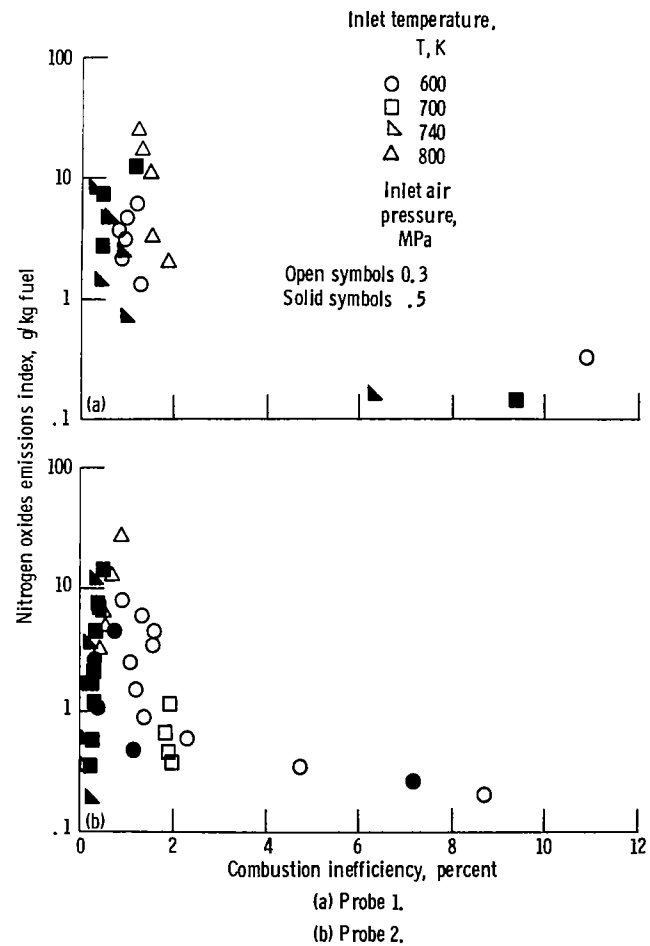


Figure 14. - Effects of inlet air pressure on emissions results. High flameholder blockage; reference velocity, 25 m/sec.

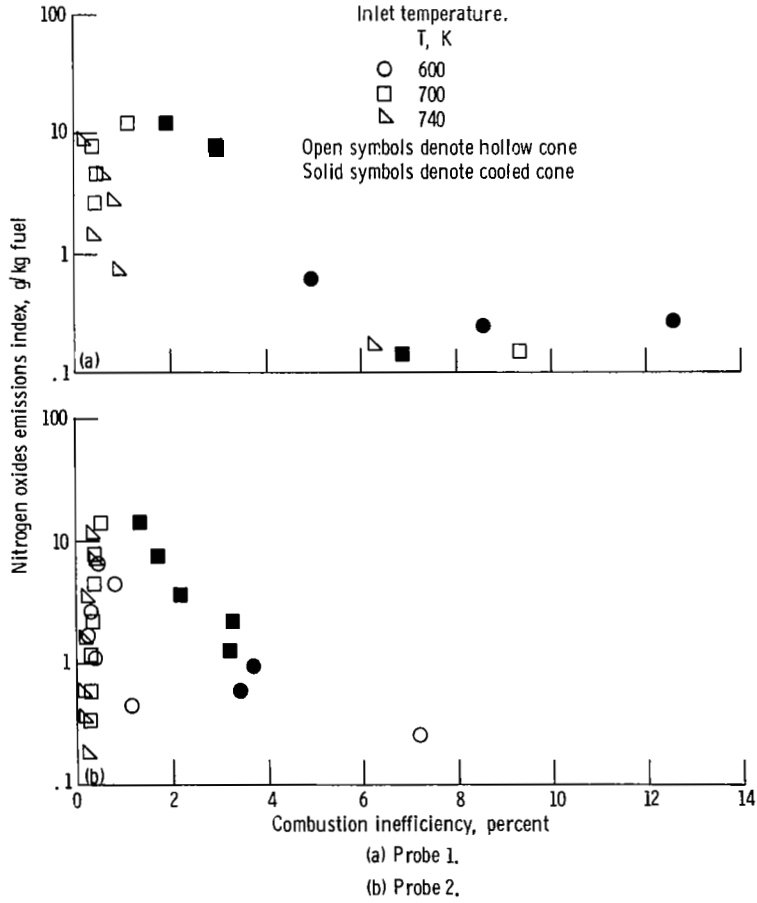


Figure 15. - Effects of water cooling of flameholder on emissions results: high blockage flameholder, inlet air pressure, 0.5 MPa; reference velocity, 25 m/sec.

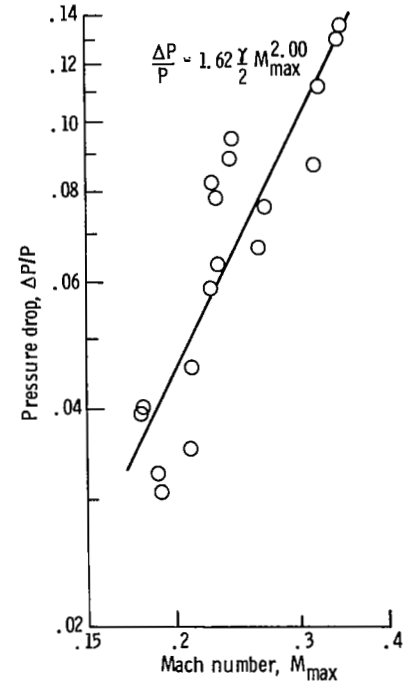


Figure 16. - Correlation of flameholder pressure drop with flameholder Mach number.

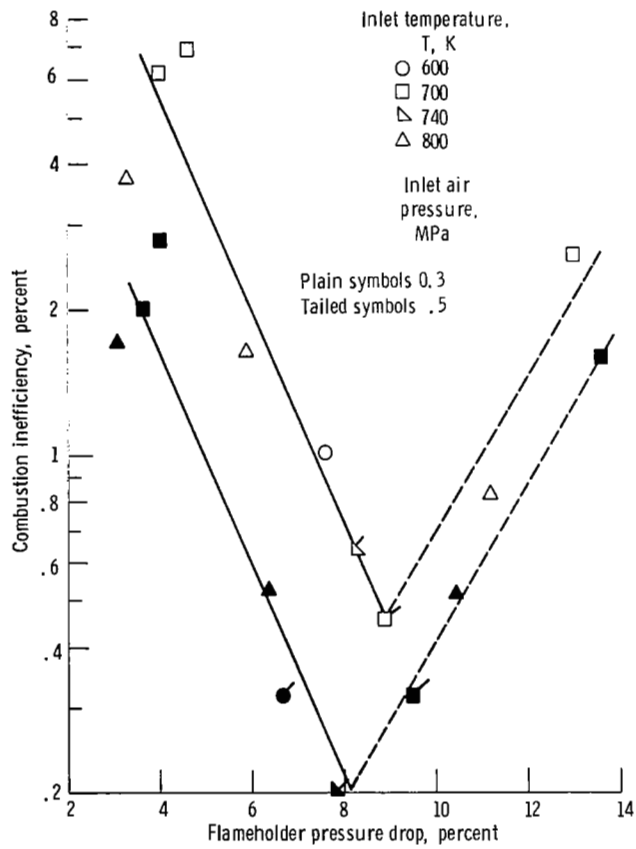


Figure 17. - Correlation of combustion inefficiency with flameholder pressure drop for equivalence ratio of 0.6.

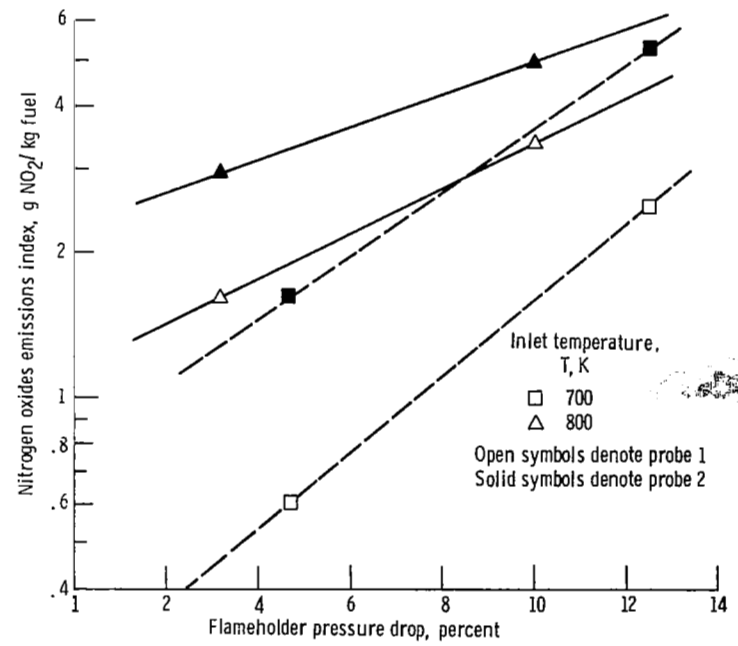


Figure 18. - Nitrogen oxides emissions index as function of flameholder pressure drop for equivalence ratio of 0.6. Inlet air pressure, 0.3 MPa; reference velocity, 35 m/sec.

1. Report No. NASA TP-2131		2. Government Accession No.		3. Recipient's Catalog No.	
4. Title and Subtitle <b>EFFECT OF FLAMEHOLDER PRESSURE DROP ON EMISSIONS AND PERFORMANCE OF PREMIXED-PREVAPORIZED COMBUSTORS</b>				5. Report Date April 1983	
				6. Performing Organization Code <b>505-32-32</b>	
7. Author(s) <b>Robert A. Duerr and Valerie J. Lyons</b>				8. Performing Organization Report No. <b>E-1358</b>	
9. Performing Organization Name and Address <b>National Aeronautics and Space Administration Lewis Research Center Cleveland, Ohio 44135</b>				10. Work Unit No.	
				11. Contract or Grant No.	
12. Sponsoring Agency Name and Address <b>National Aeronautics and Space Administration Washington, D. C. 20546</b>				13. Type of Report and Period Covered <b>Technical Paper</b>	
				14. Sponsoring Agency Code	
15. Supplementary Notes					
16. Abstract <p>Parametric tests were conducted to determine the effects of flameholder pressure drop on the emissions and performance of lean premixed-prevaporized combustors. A conical flameholder mounted in a diverging duct was tested with two values of flameholder blockage. Emissions of nitrogen oxides, carbon monoxide, carbon dioxide, and unburned hydrocarbons were measured for combustor entrance conditions of 600 to 800 K air temperature, 0.3- to 0.5-MPa pressure, and 20- to 35-m/sec reference velocity. Jet A fuel was injected at flow rates corresponding to an equivalence ratio range from 0.8 down to the lean stability limit. Emission results for the high-blockage flameholder were a substantial improvement over the low-blockage emission results. A correlation of combustion efficiency with flameholder pressure drop was developed for pressure drops less than 9 percent.</p>					
17. Key Words (Suggested by Author(s)) <b>Combustion; Flameholder; Emissions; Gas turbines; Combustor; Pressure drop</b>			18. Distribution Statement <b>Unclassified - unlimited STAR Category 07</b>		
19. Security Classif. (of this report) <b>Unclassified</b>		20. Security Classif. (of this page) <b>Unclassified</b>		21. No. of Pages 22	22. Price* A02